Tecnociencia, Vol. 26, N°2: 110-125
Julio-Diciembre 2024
ISSN L 2415-0940

SIMPLE AND LOW-COST SYNTHESIS OF LI_2FESIO_4 CATHODE MATERIALS BY MECHANICAL ACTIVATION USING A Fe^{3+} PRECURSOR

SÍNTESIS SIMPLE Y DE BAJO COSTO DE MATERIALES DE CÁTODOS DE LI_2FESIO_4 MEDIANTE ACTIVACIÓN MECÁNICA UTILIZANDO UN PRECURSOR DE Fe^{3+}

Juan Antonio Jaén
Universidad de Panamá, Facultad de Ciencias Naturales, Exactas y Tecnología, Departamento de Química Física, Panamá.
juan.jaen@up.ac.pa https://orcid.org/0000-0001-7069-216X

Ian Mendoza
Universidad de Panamá/Facultad de Ciencias Naturales, Exactas y Tecnología, Escuela de Física, Panamá.
ian.mendoza5.im@gmail.com https://orcid.org/0009-0007-0958-5470

Eduardo Chung
Universidad de Panamá, Facultad de Ciencias Naturales, Exactas y Tecnología, Departamento de Física, Panamá.
eduardo.chungng@up.ac.pa https://orcid.org/0000-0003-2834-9450

Fecha de recepción: 7 de marzo de 2024
Fecha de aceptación: 25 de abril de 2024

DOI HTTPS://DOI.ORG/10.48204/J.TECNO.V26N2.A5405

ABSTRACT

An easy and low-cost synthesis of monoclinic Li_2FeSiO_4 based on a carbothermal process and a short-time preliminary milling of a reactant mixture in a planetary mill was investigated. Monoclinic Li_2FeSiO_4/C is prepared using Fe^{3+} (Fe_2O_3) as a precursor. For this purpose, commercial hematite and one obtained through a green route were used. This material is studied and compared with Li_2FeSiO_4 obtained using Fe^{2+} ($FeC_2O_4 \cdot 2H_2O$) as a precursor. In all cases, citric acid was used as a reducing agent and as an *in situ* conductive additive. Mössbauer spectroscopy was used as the central technique in this study.

KEYWORDS

Königsberg bridges, graphic schema theory, mathematical education

RESUMEN

Se investigó la síntesis del Li_2FeSiO_4 monoclínico mediante un proceso carbotérmico posterior a una molienda preliminar de corta duración de la mezcla de los reactantes, en un molino planetario, como una forma fácil y de bajo costo para obtenerlo. El Li_2FeSiO_4/C monoclínico se preparó usando Fe^{3+} (Fe_2O_3) como precursor. Para esto, se utilizó una hematita comercial y una obtenida mediante una ruta verde. Se examinaron y se compararon con Li_2FeSiO_4 obtenido usando Fe^{2+} ($FeC_2O_4 \cdot 2H_2O$) como precursor. En todos los casos se utilizó ácido cítrico como agente reductor *in situ* y como un aditivo conductor. Se usó espectroscopía Mössbauer como técnica central en este estudio.

PALABRAS CLAVES

Puentes de Königsberg, teoría de grafos, Educación Matemática

INTRODUCTION

Li_2FeSiO_4 has been considered an attractive cathode material for rechargeable lithium batteries since it possesses high theoretical capacity (approximately 331 $mAh \cdot g^{-1}$), good thermal stability and cycling performance, nontoxicity, environmental friendliness, and is of low cost (Nytén et al., 2005; Guirish & Shao, 2015; Fujita et al., 2018). Many synthesis procedures have been proposed and used, such as the solid-state method, sol-gel technique, hydrothermal/solvothermal/supercritical fluid techniques, microwave method, spray pyrolysis/combustion/hydro-chemical techniques, polyol process and ionothermal techniques (Guirish & Shao, 2015; Ferrari et al., 2014). The mechanical activation reaction method is appropriate for large-scale production, but the impurities such as iron oxides, metallic iron, and lithium silicates, the larger particle size of the final product, and agglomerations could not be easily avoided. This has negative effects on the electrochemical performances of the products. The carbothermal reduction method is an efficient synthetic method to obtain metal or low-valent metallic oxide, and it has been applied to the synthesis of $LiFePO_4$/C and Li_2FeSiO_4/C.

Most of the recent synthesis procedures are designed to optimize the intrinsic and extrinsic properties of Li_2FeSiO_4 by applying grain size reduction, morphology control, doping with some transition metal cations in Fe and Si sites, and conductive carbon coating, among others (Yi et al., 2017). Unfortunately, there remain difficulties in synthesizing a single-phase material. The potential and the low-cost advantage are not realized if expensive Fe^{2+} precursor compounds are used as the starting materials in the synthesis procedures. There are, however, some examples where Li_2FeSiO_4/C cathode material is successfully synthesized from Fe_2O_3 (Table 1).

In the present study, an easy and low-cost synthesis of Li_2FeSiO_4 was investigated using a Fe^{3+} precursor based on short-time preliminary milling of a reactant mixture in a planetary mill followed by calcination.

EXPERIMENTAL METHODS

Synthesis

Li_2FeSiO_4 was synthesized by ball milling-assisted solid-state reaction using $FeC_2O_4 \cdot 2H_2O$ (iron II oxalate), 500 mesh commercial Fe_2O_3 (hematite), and synthesized hematite by a green route.

- **Using Iron II oxalate as a precursor**

Dehydrated Iron II oxalate (Aldrich Chemistry, 99%), lithium silicate (GFS Chemicals, ≥99.5%), and typically 1.50 g of citric acid ($C_6H_8O_7$) with 15%w/w was ball milling using low energy for 36 hours with two different rpm´s (250 and 300) and hardened steel balls per gram of mixture 15:1 mass ratio. Solid-state reactions were carried out at 400°C for 2 hours and two different calcination temperatures (700°C and 750°C) for different calcination times in an inert Argon gas atmosphere.

- **Using Commercial Hematite 500 Mesh as a precursor**

500 mesh hematite (Applichem CAS1309-37-1) was ball milled at low energy (15:1 mass ratio) for 24 hours with 250 rpm, before mixing with other components. Then, a mixture of hematite, lithium silicate, and citric acid in stoichiometric amounts with 32% w/w was ground and mixed in an agate mortar. The mixture was calcinated at 400°C for 4 hours followed by calcination at 750°C for 10 hours, all in an Argon gas inert atmosphere. Also, a paste was formed by adding methanol to the reaction mixture and was ball milled for 24 hours using low energy conditions (250 rpm, ball/mass ratio 15:1) and then calcinated for 2 hours at 400°C, followed by 10 hours of calcination at 700°C/7050°C, all in an inert atmosphere of Argon gas.

- **Using Hematite obtained by a green route.**

The above procedure was repeated using hematite obtained by a green route (Freire et al., 2023). When heating the amorphous iron oxide precipitated from the methanolic *Caesalpinia coriaria* (Jacq.) Willd. fruits extract, hematite is obtained.

Characterization techniques

XRD measurements were performed in X-ray diffraction (PANalytical X'Pert powder diffractometer, Cu K_α radiation) in the range of $10° \leq 2\Theta \leq 80°$ at intervals of 0.02° in Bragg-Brentano geometry. The attenuated total reflection Fourier transform infrared (ATR-FTIR) spectra were recorded in the 4000-300 cm^{-1} range on an FTIR Frontier de Perkin Elmer spectrophotometer with ATR. A resolution of 2 cm^{-1} was used to obtain all the spectra. The room temperature Mössbauer spectra for all samples were collected in a spectrometer working at the standard transmission geometry by moving the vibrator with a triangular reference signal. A $^{57}Co/Rh$ source of 10 mCi (925 MBq) of nominal activity was used. The spectrometer was regularly calibrated by collecting the RT Mössbauer spectrum of a standard

α-Fe foil. All spectra were fitted by using a Lorentzian or Voigt-based routine of the Recoil software (University of Ottawa, Canada).

Table 1.
Summary of Li_2FeSiO_4/C cathode material is successfully synthesized from Fe_2O_3.

Synthesis method	Raw materials	Annealing conditions	Phase structure	Impurities	References
Ball milling (400 rpm, 10h) / heat treatment	Li_2CO_3, Fe_2O_3, $(C_2H_5O)_4Si$ and Sucrose (10 wt%)	600 °C, 12 h (N_2)	Orthorhombic $Pmn2_1$	Li_2SiO_3, Fe_3O_4	Zhang et al., 2013
Sol-gel (hydrothermal)	$LiCH_3COO{\cdot}2H_2O$, Synthetic Fe_2O_3 (cubic, spherical, and commercial nano), tetraethyl orthosilicate, and citric acid	350 °C, 2h /700 °C, 10 h (Ar)	Monoclinic $P2_1$	None	Yi et al., 2017
Solid state (ground in an agate mortar)	Li_2SiO_3, Fe_2O_3, and glucose (19 and 38 wt.%)	700 °C, 7 h (Ar)	Monoclinic $P2_1/n$	Li_2SiO_3, Fe_3O_4, FeO, Fe	Kalantarian et al., 2017
Sol-gel	Lithium acetate, iron(III) nitrate, tetra-ethyl orthosilicate (TEOS) ethylene glycol and citric acid	700 °C, 7 h (Ar)	Monoclinic $P2_1/n$	Halite (NaCl)	Kalantaria et al., 2017
Sol-gel	Synthetic Fe_2O_3 microsphere, $LiCH_3COO{\cdot}\ 2H_2O$ and tetra-ethyl orthosilicate (TEOS)	700 °C, 7 h (Ar)	Orthorhombic $Pmn2_1$	None	Qu et al., 2012; Qu et al., 2013

RESULTS AND DISCUSSION

Li_2FeSiO_4 using $FeC_2O_4 \cdot 2H_2O$ as precursor

The XRD pattern of powders obtained from mechanical milling is shown in Fig. 1.

Figure 1.
Diffraction patterns of the precursors a) Li_2SiO_3 and b) $FeC_2O_4 \cdot 2H_2O$, and c) the mixture of milled powders using the oxalate precursor technique.

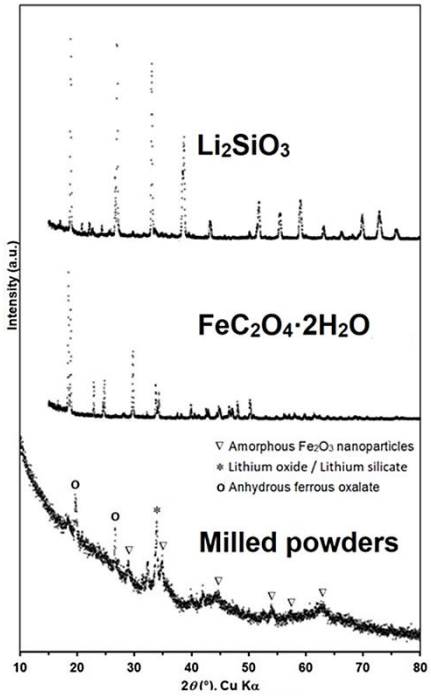

The transformation of the precursors Li_2SiO_3 and $FeC_2O_4 \cdot 2H_2O$ is clearly seen, whose diffractograms are given in Fig. 1 (a) and (b). New weak and broad reflections are assigned to a mixture of anhydrous ferrous oxalate FeC_2O_4 (Brown & Bevan, 1966; Hermanek et al., 2007). Li_2SiO_3, and a phase designated as amorphous nanoparticles of F_2O_3 in correspondence with the Mössbauer data that is provided later. According to the X-ray, milling results in the amorphization and initial interaction of precursor materials, with the formation of an intermediate product of reduced particle size.

The transmission Mössbauer spectrum of the ball milled sample, exhibited in Fig. 2a, was fitted using a two-component model. The less intense doublet had a quadrupole splitting (QS) of 2.11 $mm \cdot s^{-1}$and isomer shift (IS) of 1.23 $mm \cdot s^{-1}$ (see Fig. 2a).

Figure 2.
ATR-FTIR spectrum of the milled powders using the oxalate precursor technique.

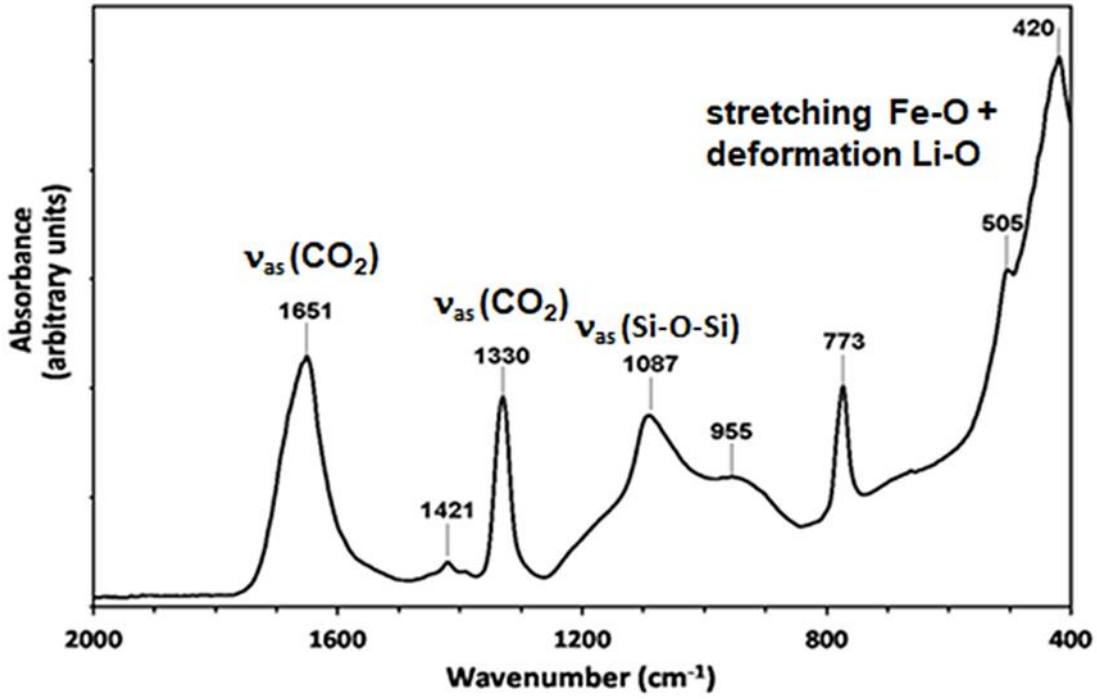

This quadrupole splitting value was consistent with an electron configuration of high spin for the Fe (II) cation and the isomer shift value was in the range expected for Fe (II) in octahedral or quasi-octahedral environments (Drago, 1965). This doublet was assigned to anhydrous ferrous oxalate, in accordance with studies on the thermal decomposition of $FeC_2O_4 \cdot 2H_2O$ (Cari et al., 1975; Smrčka et al., 2016). The second doublet was fitted by using an IS of 0.36 mm·s^{-1} and QS of 0.76 mm·s^{-1}, typical of high spin Fe^3 ions in octahedral coordination, which could be assigned ions in octahedral coordination, which could be assigned to amorphous nanoparticles of Fe_2O_3 (Smrčka et al., 2016; Milivojevi et al., 2014; Machala et al., 2007). Thus, Mössbauer suggests an amorphous character for this phase of Fe_2O_3. If the crystal size is about 5-6 nm, XRD will not distinguish the nanocrystals of iron oxide (III), but Mössbauer will.

Figure 2 shows the infrared FTIR-ATR spectrum of the powders (oxalate technique) after the mechanical milling of the precursors. This profile is not related to those of the precursors. Several of the observed bands can be assigned to the oxalate anion since they coincide with well-known data on vibratory frequencies of spectroscopic studies of a large variety of metal oxalates (Dinnebier et al., 2003; Begun & Fleter, 1963). The peaks at 1651 cm^{-1} 1330 cm^{-1}

and 773 cm^{-1} are interpreted as a result of vibrational modes of iron oxalate (II) (FeC_2O_4) in the solid state in which the oxalate anion is placed in a C_{2h} symmetry site in the crystal structure. The peaks at 1651 cm^{-1} and 1330 cm^{-1} corresponded to asymmetric vibrations ν_{as} (CO_2) the peak at 773 cm^{-1} was due to the asymmetric flex δ (CO_2) (Dinnebier et al., 2003;). The rest of the spectrum of this spectrum could be associated with the presence of amorphous iron oxide (Raman et al., 1991) and Li_2SiO_3 (Zhang et al, 2008; Cruz & Bulbulian, 2005; Yang et al., 2013). The signal at 955 cm^{-1} may be related to vibrations O-Si-O, while the absorption at 505 cm^{-1} can be due to a stretching band Fe-O and deformation Si-O-Li.

Figure 3 shows the evolution of the room temperature Mössbauer spectra of the milled powders heat-treated at 705 ° C for different times. The spectrum of the sample heated for two hours (see Figure 2b) consisted of a slightly asymmetric doublet and a sextet with broad lines. The doublet had hyperfine parameters (IS = 0.24 $mm \cdot s^{-1}$ and QS = 0.69 $mm \cdot s^{-1}$) typical of the superparamagnetic Fe_2O_3. The broadened sextet with B = 47.9 T, IS= 0.28 $mm \cdot s^{-1}$, and QS = -0.01 mm·s-1 resulted from the heat treatment, which induces more crystalline Fe_2O_3.

Figure 3.
Mössbauer spectra at room temperature powders milled (oxalate precursor) and thermally treated at 705 °C in Ar atmosphere for a) 0 h, b) 2 hours, c) 6 hours, d) 10 hours, and e) 20 hours

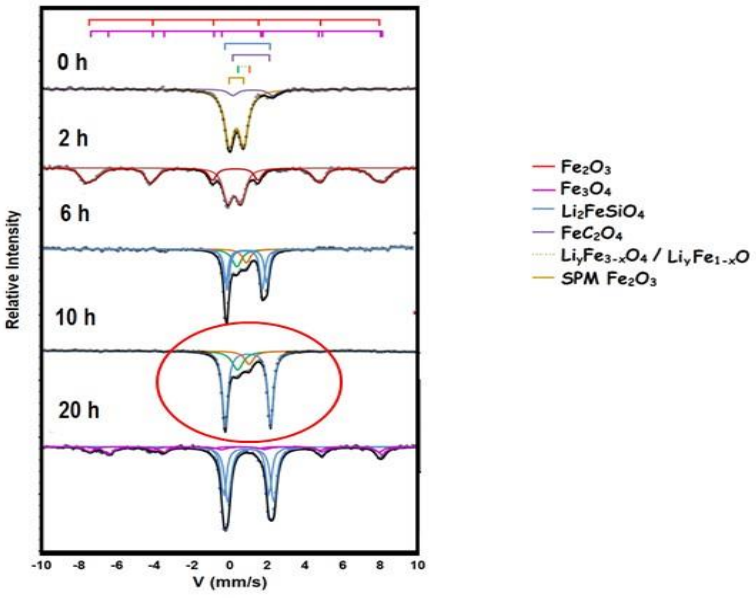

The thermal treatment at 705°C for periods longer than 6 hours results in samples whose Mössbauer spectra have a central doublet, clearly of high spin Fe^{2+} in the tetrahedral coordination. The similarity in the position of the spectral lines of the doublet suggests similar local environments for the Fe. However, the values of the quadrupole splitting are significantly different between the samples. According to (Mali et al., 2011), the values of the quadrupole splitting can be strongly correlated with the degree of distortion of the FeO_4 tetrahedra in the orthosilicates. In the sample heated for 6 hours, it was fitted with two quadrupole sites with QS values of 1.88 $mm \cdot s^{-1}$ and 2.19 $mm \cdot s^{-1}$. The doublet in the spectra of samples heated for 10 hours, has a QS ~ 2.42 $mm \cdot s^{-1}$, which coincided with those of the monoclinic structure *P2₁/n* of the lithium iron orthosilicate, Li_2FeSiO_4 (Jugović et al., 2014; Lv et al., 2011; Sirisopanaporn et al., 2010; Dominko, 2008). is noteworthy that by carefully controlling the experimental conditions, the purity of the ball-milled synthesized orthosilicate Li_2FeSiO_4 can be improved, A sample obtained using 300 RPM during milling, exhibits a Mössbauer spectrum consisting of two sets of Fe^{2+}+ and Fe^{3+} doublets as depicted in Figure 4, a prominent one belonging to the lithium iron orthosilicate doublet (CS = 0.947(1) mm/s and QS = 2.400(2) mm/s) and a very small one (CS = 0.29(5) mm/s and QS = 0.88(9) mm/s) which is attributed to delithiated lithium iron orthosilicate $Li_{2-x}FeSiO_4$ (Kyu Lee et al., 2013; Nytén et al., 2006).

Figure 4.
Mössbauer spectrum at room temperature of a lithium iron orthosilicate obtained using 300 rpm during ball milling.

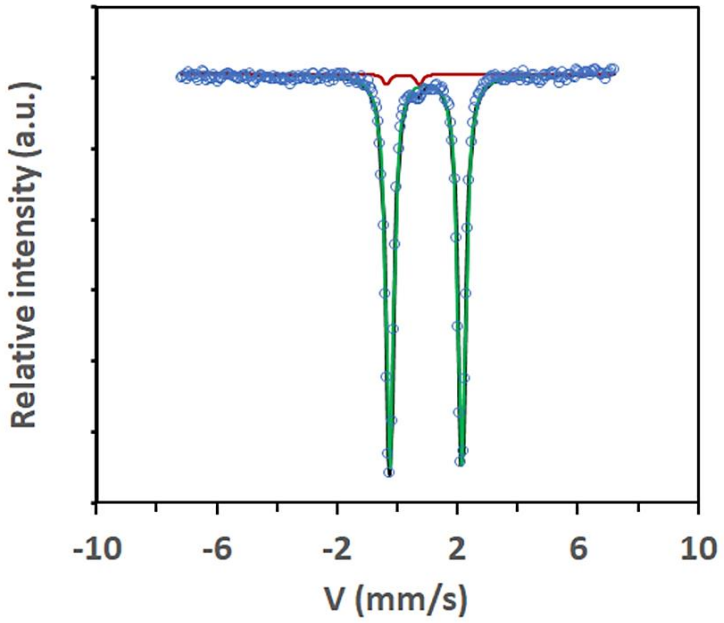

The delithiated orthosilicate $Li_{2-x}FeSiO_4$ is in very small quantities, so is difficult to clearly observe it in the XRD. It is interesting to point out that neither Fe^0 impurities nor other iron oxides (lithiated magnetite and lithiated wustite) were observed in the spectrum of some samples heated for 20 hours, which in turn exhibited a smaller contribution to two magnetic sextets that may be attributed to non-stoichiometric magnetite, $Fe_{3-x}O_4$.

The milling causes the dehydration of ferrous oxalate and simultaneously, an atmosphere is generated that leads to the formation of amorphous nanoparticles of Fe_2O_3, like what happens during the thermal decomposition of oxalate. It is interesting to observe that from the pure divalent state of Fe^{2+} in FeC_2O_4, it converts to the trivalent state Fe^{3+} in mechanical milling, even in an argon atmosphere. The transformations can be described by the equations.

$$FeC_2O_4 \cdot 2H_2O \rightarrow FeC_2O_4 + 2\ H_2O \quad (1)$$
$$2\ FeC_2O_4 \rightarrow Fe_2O_3 + CO_2 + 3\ CO \quad (2)$$
$$2\ FeC_2O_4 \cdot 2H_2O \rightarrow Fe_2O_3 + 2\ H_2O + 3\ CO_2 + CO + 2H_2 \quad (3)$$

The formation of other oxides is induced during the first part of the heat treatmentat at 400 °C.

$$FeC_2O_4 \rightarrow FeO + CO + CO_2 \quad (4)$$
$$3\ FeC_2O_4 \rightarrow Fe_3O_4 + 2\ CO_2 + 4\ CO \quad (5)$$
$$Fe_3O_4 + CO \rightarrow 3\ FeO + CO_2 \quad (6)$$

Frecuently, the formation of metallic iron is observed after heat treatment.

$$Fe_2O_3 + 3\ C \rightarrow 2\ Fe + 3\ CO \quad (7)$$
$$FeO + CO \rightarrow Fe + CO_2 \quad (8)$$
$$4FeO \rightarrow Fe_3O_4 + Fe \quad (9)$$
$$Li_2FeSiO_4 + C \rightarrow Fe + CO + Li_2SO_3 \quad (10)$$

In the above discussion, it should be emphasized that the amorphous nanoparticles Fe_2O_3 react with Li_2SiO_3 after the intermediate step at 410 °C, so that the product of the solid-state reaction at temperatures around 705 °C is the orthosilicate Li_2FeSiO_4, the monoclinic polymorph (space group: *P21/n*).

Li_2FeSiO_4 using commercial Fe_2O_3 as precursor

The spectrum of the product obtained without milling is shown in Figure 5 (a). Three contributions is clearly observed. One doublet indicative of iron ions in a trivalent oxidized state (CS_1=0.59 ± 0.02 mm/s, QS_1 = 0.64 ± 0.02 mm/s, the second doublet with Mössbauer parameters CS_2=0.83 ± 0.02 mm/s, QS_2 = 0.76 ± 0.02 mm/s), and a third one, belonging to a

divalent oxidized state contributing with 24% to the spectral area, with CS = 0.959(4) mm/s and QS = 2.449(9) mm/s. The last doublet evidently is due to the formation of the lithium iron orthosilicate phase through a solid-state reaction. When ball milling is used in the synthesis procedure,

When the reaction mixture is ball-milled at 250 rpm, the Mössbauer spectrum typically consists of two doublets (Figure (5b)). One doublet indicative of iron ions in a trivalent oxidized state (CS_1=0.265(5) mm/s, QS_1 = 0.73(8)mm/s, while the majority phase exhibiting a doublet with Mössbauer parameters CS_2=0.958(4), QS_2 = 2.431(7) is attributed to the divalent oxidized phase of lithium iron orthosilicate, Li_2FeSiO_4 (Jugović et al., 2014; Lv et al., 2011; Sirisopanaporn et al., 2010; Dominko. 2008). This result demonstrates that by introducing milling in the synthesis procedure leads to the desired formation of Li_2FeSiO_4. As in the case of samples obtained using oxalate precursors, the small area contribution may come from delithiated orthosilicate $Li_{2-x}FeSiO_4$. In this last spectrum, traces of a magnetic components are observed. A sufficient electric conductivity is expected, with electrochemical performance comparable with Li_2FeSiO_4 prepared from Fe^{2+} precursor.

Figure 5.
Mössbauer spectrum at room temperature of a lithium iron orthosilicate obtained using hematite as a precursor of (a) unmailed sample, (b) ball-milled sample (250 rpm) prepared with commercial Fe_2O_3, and (c) ball-milled sample (250 rpm) prepared with green route Fe_2O_3.

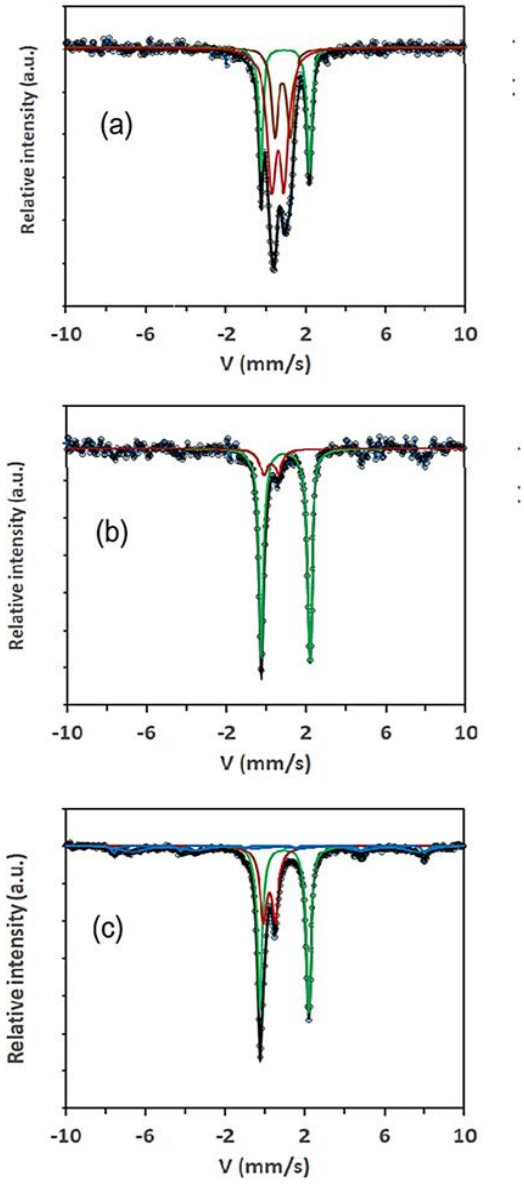

One should carefully observe the experimental synthesis conditions. This is illustrated in Figure 6, which shows the room-temperature Mössbauer spectrum of a sample obtained using a reduced amount of citric acid, 1.14 g instead of 1.50 g. Because of the reducing power diminishes, large concentrations of magnetite are obtained. Decreasing the grinding time (e.g., 10 h) also causes the formation of magnetite, although in a much smaller quantity.

Figure 6.
Mössbauer spectrum at room temperature of a sample obtained using commercial Fe_2O_3 as a precursor, a ball-milling procedure (250 rpm), and only 1.14 g of citric acid.

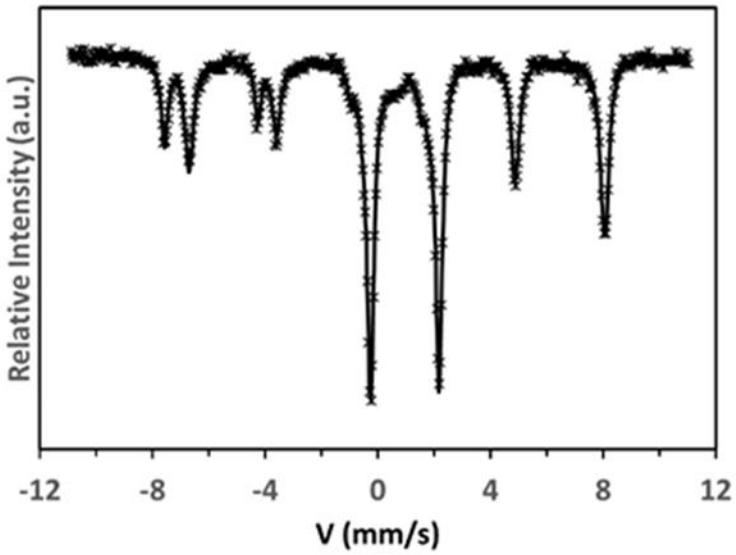

Li_2FeSiO_4 using green route obtained Fe_2O_3 as the precursor.
As expected, the products obtained using hematite synthesized by a green route are quite similar to those using commercial hematite. The Mössbauer spectrum of a ball milled at 250 rpm sample also exhibits two doublets. The doublet corresponding to the lithium iron orthosilicate phase, the majority phase, has hyperfine parameters CS = 0.959(2) mm/s; QS = 2.439(4) mm/s. The subspectrum of the delithiaded orthosilicate, $Li_{2-x}FeSiO_4$, has parameters CS = 0.216(5) mm/s; QS = 0.589(8) mm/s, but in this case, it appears in a greater proportion due to the smaller particle size. Delithiation occurs on the surface of the particle, so the surface/bulk ratio is greater in these samples. The spectrum also shows the contribution of some magnetite in the sample.

CONCLUSION

Ball mill-assisted solid-state carbothermal synthesis of Li_2FeSiO_4 using Fe_2O_3 in an inert atmosphere is feasible. A homogeneous, crystalline Li_2FeSiO_4 is formed after brief annealing at temperatures of 700°C - 750°C, but preliminary milling is required to improve the amounts of orthosilicate formed,

Obtaining impurities such as Fe_xO, Fe_3O_4, and delithiated $Li_{2-x}FeSiO_4$ continues to be a problem. Improving the synthesis procedure is required. For example, controlling the amount of citric acid is necessary to ensure the reduction of Fe^{3+} to Fe^{2+}. The added carbon, in the form of citric acid, acts as a reducing and covering agent, resulting in the formation of fine particulate Li_2FeSiO_4.

The carbothermal synthesis of Li_2FeSiO_4 using low-cost and readily available Fe_2O_3 and a previous low-energy mechanical alloying process is a convenient and ecologically clean method with a reduced material cost.

BIBLIOGRAPHIC REFERENCES

Begun, K.M., & W.H. Fletcher. 1963. Vibrational spectra of aqueous oxalate ion. Spectrochim Acta. 19: 1343-1349

Brown, R.A., & S.C. Bevan. 1966 The thermal decomposition of ferrous oxalate dehydrate. J Inorg Nucl Chem 28: 387-391

Carić S., J. Marinkov, & A. Slivka. 1975. Mössbauer Study of the Thermal Decomposition of FeC2O4·2H2O. Phys Stat Sol 31(1): 263–

Cruz D., S. Bulbulian. 2005. Synthesis of Li4SiO4 by a Modified Combustion Method. J Am Ceram Soc 88(7): 1720-1724

Dinnebier R., S. Vensky S, M. Panthöfer, & M. Jansen. 2003. Molecular Structures of Alkali Oxalates: First Proof of a Staggered Oxalate Anion in the Solid State. Inorg Chem 42(5): 1499−1507

Dominko, R. 2008. Li2MSiO4 (M = Fe and/or Mn) cathode materials. J Power Sources 184(2): 462−468

Drago, R.S. 1965. Physical Methods in Inorganic Chemistry. Reinhold Publ, New York

Ferrari S., D. Capsoni, S. Casino, M. Destro, C. Gerbaldi, & M. Binia. 2014. Electrochemistry of orthosilicate-based lithium battery cathodes: a perspective. Phys. Chem. Chem. Phys. 16:10353-10366

Freire, A., E. Chung, I. Mendoza, & J.A. Jaén. 2023. Green synthesis of iron oxide nanoparticles using Caesalpinia coriaria (Jacq.) Willd. fruits extract. Hyperfine Interact 244, 6. https://doi.org/10.1007/s10751-023-01817-6

Fujita Y., T. Hira, K. Shida, M. Tsushida, J. Liao, & M. Matsuda. 2018. Microstructure of high battery-performance Li2FeSiO4/C composite powder synthesized by combining different carbon sources in spray-freezing/freeze-drying process. Ceram. Int. 44: 11211–11217

Guirish H.N., & G. Shao. 2015. Advances in high-capacity Li2MSiO4 (M = Mn, Fe, Co, Ni, …) cathode materials for lithium-ion batteries. RSC Adv. 5:98666-98686

Hermanek M., R. Zboril, I. Medrik, J. Pechousek, & C. Gregor. 2007. Catalytic Efficiency of Iron (III) Oxides in Decomposition of Hydrogen Peroxide: Competition between the Surface Area and Crystallinity of Nanoparticles. J Am Chem Soc 129(35): 10931-10936

Jugović D, M. Milović, VN Ivanovski, M. Avdeev, RB. Dominko, B. Jokić, & D. Uskokovi. (2014) Structural study of monoclinic Li2FeSiO4 by X-ray diffraction and Mössbauer spectroscopy. J Power Sources 265: 75-80. https://doi.org/10.1016/j.jpowsour.2014.04.121

Kalantarian M. M., M. Oghbaei, S. Asgari, L. Karimi, S. Ferrari, D. Capsoni, M. Bini, & P. Mustarelli. 2017. Electrochemical Characterization of Low-Cost Lithium-Iron Orthosilicate Samples as Cathode Materials of Lithium-Ion Battery. Adv. Ceram. Prog 3, 19-25.

Lee K, S.J. Kim, T. Kouh, & C.S. Kim. 2013. Mössbauer analysis of silicate Li2FeSiO4 and delithiated Li2−xFeSiO4 (x=0.66) compounds. J. Appl. Phys. 113, 17E306. http://dx.doi.org/10.1063/1.4799153

Lv D., W. Wen, X. Huang, J. Bai, J. Mi, S. Wu, & Y. Yang. 2011. A novel Li2FeSiO4/C composite: Synthesis, characterization and high storage capacity. J Mater Chem 21: 9506-9512

Machala L., R. Zboril, & A. Gedanken. 2007. Amorphous Iron (III) Oxides. J Phys Chem 111: 4003-4018 Decomposition of FeC2O4·2H2O. Phys Stat Sol 31(1): 263–268

Mali G., C. Sirisopanaporn, C. Masquelier, D. Hanzel, & R. Dominko. 2011. Li2FeSiO4 polymorphs probed by 6Li MAS NMR and 57Fe Mössbauer spectroscopy. Chem Mater 23: 2735–27448

Milivojević D., B. Babić-Stojić, V. Jokanović, Z. Jagličić, D. Makovec, & N. Jović. 2014. Magnetic properties of ultrasmall iron-oxide nanoparticles. J Alloys Compd 595: 153-157

Nytén A., S. Kamali, L. Hägström, T. Gustafsson, & J.O. Thomas. 2006. The lithium extraction/insertion mechanism in Li2FeSiO4. J. Mater. Chem., 16, 2266–2272

Nytén A., A. Abouimrane, M. Armand, T. Gustafsson T, & J.O. Thomas. 2005. Electrochemical performance of Li2FeSiO4 as a new Li-battery cathode material. Electrochem Commun 7:156−160

Qu L., S. Fang, Z. Zhang, L. Yang, & S. Hirano. 2013. Li2FeSiO4/C with good performance as cathode material for Li-ion battery Mater. Lett. 108, 1–4. https://doi.org/10.1016/j.matlet.2013.06.072

Qu, L., S. Fang, L. Yang, & S. Hirano. 2012. LI2FeSiO4/C cathode material synthesized by template-assisted sol–gel process with Fe2O3 microsphere. Journal of Power Sources, 217, 243–247. https://doi.org/10.1016/j.jpowsour.2012.05.093

Raman A., B. Kuban, & A. Razvan.1991. The Application of Infrared Spectroscopy to the Study of Atmospheric Rust Systems-I Standard Spectra and Illustrative Applications to Identify Rust Phases in Natural Atmospheric Corrosion Products. Corros Sci 32(12): 1295-1306

Sirisopanaporn C., A. Boulinea, D. Hanzel, R. Dominko, B. Budic, A.R. Armstrong, P.G. Bruce, & C. Masquelier. 2010. Crystal structure of a new polymorph of Li2FeSiO4. Inorg Chem 49: 7446−7451

Smrčka D., V. Procházka, P. Novák, J. Kašlík, & V. Vlastimil. 2016. Iron oxalate decomposition process by means of Mössbauer spectroscopy and nuclear forward scattering. AIP Conf Proc 1781-1789

Yang H., Y. Zhang, X. Cheng. 2013. Effect of Vanadium Substitution on Structure of Li2FeSiO4/C Composites. J Electrochem 19(6): 565-570

Yi, L., G. Wang, Y. Bai, M. Liu, X. Wang, M. Liu, & X. Wang. 2017. The effects of morphology and size on performances of Li2FeSiO4/C cathode materials. Journal of Alloys and Compounds, 721, 683–690. https://doi.org/10.1016/j.jallcom.2017.06.059

Zhang B., M. Nieuwoudt, & A. Easteal. 2008. Sol Gel Route to Nanocrystalline Lithium Metasilicate Particles. J Am Ceram Soc 91(6): 1927–193

Zhang, Z., X. Liu, S. Ma, & H.Y. Zhao. 2013. Preparation of Li2FeSiO4/c composite cathode materials for lithium-ion batteries by Carbothermal Reduction Method. Adv. Mater. Res. 724-725, 838–843. https://doi.org/10.4028/www.scientific.net/amr.724-725.838